Nanosystem Similarity: Modeling and Comparison of Amphiphilic Monolayers Adsorbed on Nanorough Surfaces

Axel Drefahl,* Olaf Seidel, and Hans-Jörg Mögel

Insitute of Physical Chemistry, Freiberg University of Mining and Technology, 09596 Freiberg, Germany

Received April 15, 1998

The similarity concept and its potential application to nanosystems including tenside-solvent-particle, TSP, systems is discussed. In addition, TSP systems are simulated with the Monte Carlo approach. We model TSP systems on a coarse-grained lattice in which tenside molecules are represented as amphiphilic chains with one hydrophilic head and with several hydrophobic tail segments. We apply the random walk approach to the modeling of grafted amphiphilic molecules with flexible chains. Mean amphiphile properties are calculated employing the Monte Carlo technique to systems with planar and with nanorough surfaces. Surfaces of different roughness and with various topography are generated by application of deposition models. The influence of surface properties on amphiphilic monolayer properties is investigated. In particular, segment-surface contact probabilities are discussed as a function of surface properties and amphiphile chain length. We have found that the segments next to the head segments have the largest contact probability which then decreases until a minimum is reached three quarters of the chain length away from the head segment. This minimum is observed to be independent of the surface and of other monolayer properties.

INTRODUCTION

Nanosystems are molecular and supramolecular structures and devices.[1] They are characterized by properties falling into two categories. First, there are properties based on nearly independent contributions of substructural parts of the system. These properties can be calculated using group contribution models, GCM.[2−7] Advanced GCMs include various correction terms for specific intra- or intermolecular interactions, indicating that truly most of the properties belong to the second category in which properties depend on the mutual interaction of the substructural parts. Properties of "simple" systems such as gases, liquids, and solids and of complex systems including colloidal, polymeric, and biological systems are determined by intermolecular and interparticles forces.[8] Mutual interactions between substructural parts of a nanosystem lead to time-dependent microscopic changes of the nanosystem even under equilibrium conditions. Different points in time correspond to microscopically different states of the system. Molecular dynamics, MD, methods[9,10] obtain a sequence of such states by numerically solving differential equations of motion of the submolecular parts. Currently, MD simulation time, corresponding to real times of order nanoseconds, is too short to sample fully all the equilibrium fluctuations,[11a] especially in large and complex systems. With Monte Carlo, MC, methods[11−14] a collection of temporally not related microscopic states, called an ensemble, is generated randomly beginning with a start configuration and then generating each subsequent configuration from its previous configuration. Equilibrium properties of nanosystems are calculated as time and ensemble averages with the MD- and MC-method, respectively. MC-simulation, in particular, has been applied to estimate properties of large, multicomponent systems. Polymer chains,[15−41] solutions,[42−47] mixtures,[48−54] melts,[55−60] star- and hyperbranched chains[61−69] as well as amphiphiles and polymers on surfaces[70−98] have extensively been studied by MC-simulation.

In this work, we investigate the behavior of tensides. Tensides are also called surfactants.[99] The tenside molecules will be grafted onto planar and nanorough surfaces of solid particles. Such particles play a key role in environmental fate modeling and in process engineering.[100] The goal is to contribute to the understanding of particle−particle interaction. Comparison of tenside-solvent-particle, TSP, systems with less complex systems such as tenside solutions and tenside films may provide valuable data and knowledge to predict TSP system properties. In the next paragraph, we will start with a brief review on molecular and film similarity having TSP-property prediction in mind.

Tensides applied in process control are addressed as dispersants or flocculants depending on their expected function. Particle conditioning and the tendency of particles to aggregate or to disperse in a solvent is related to the film structure and the surface coverage achieved by the grafted tenside molecules.[101] The probability of contacts between the particle surface and submolecular parts of the surfactant molecules is a significant factor in governing processes with TSP-involvement. Therefore, we will evaluate segment-surface-contact, SSC, probabilities for two-dimensional (2D) single chain molecules and for three-dimensional (3D) chains in monolayers grafted onto planar and nanorough surfaces. The TSP-system will be represented by a coarse-grained model for amphiphile-surface systems. Using MC-simulation we will derive SSC and grafting probabilities and mean geometrical parameters of films on surfaces of different roughness and topography.

10.1021/ci980062x CCC: $15.00
Published on Web 10/24/1998

NANOSYSTEM SIMILARITY

Similarity is a guiding principle in both research and engineering. Progress in systematic understanding of nanosystems is achieved by investigation of novel systems that are similar to well studied reference systems. Insight into complex nanosystems may be advanced by breaking down system complexity. Thus, the similarity or dissimilarity among surfactant molecules, among nanofilms, and among surfaces are of special interest for TSP systems. Details of similarity measurements, database searching, and property estimation methods have been summarized and demonstrated elsewhere[102−106] and will not be labored in the following short review. Instead, an attempt will be made to highlight the similarity concept in context with the description and modeling of TSP systems.

Molecular Similarity. The growth of databases and information available through the World Wide Web increases the desire for extracting chemical information to answer a query in an efficient way. One may not expect the exact answer waiting at some location, but there may be a chance that information significantly related to ones query is around. Looking for molecular structures not yet synthesized, information on similar, already synthesized structures is highly profitable. Often, property data for a set of structurally related compounds are compressed into empirical quantitative structure−property relationships, QSPR, and the similarity between a query and the QSPR-compounds may provide information on whether to apply or reject a particular QSPR to the query compound. QSPRs have been compiled and discussed elsewhere.[3−7,107] Here, we will restrict ourselves by directing attention to a QSPR analysis concerning the estimation of polymer glass transition temperatures[108] and to an artificial neural network study of the clearing temperature of nematic liquid crystal systems.[109]

Measurement of the similarity between two molecules is based on the comparison of their molecular graphs by defining a similarity index as a function of selected graph and subgraph properties.[110−113] The calculation of such a similarity index is required by the *k*-nearest-neighbor method, *k*NN, applied in property estimation and compound classification[114,115] In combination with the group interchange method, GIM, *k*NN-based property estimation is enhanced by accounting for particular structural differences between query and database compounds,[116] allowing supervised, application-sensitive data evaluation, plausibility checking, and decision making. For instance, similarity or dissimilarity arguments support the selection of surfactants to optimize drug dispersion, corrosion inhibition or mineral flotation, and flocculation processes. Based on the GIM the relative difference in hydrophobicity or hydrophilicity between compounds may be calculated.[117] This approach has nicely been illustrated in qualitative terms for dodecane congeners.[118] In analogy, other surfactant properties important in process engineering such as surface tension, adsorption isotherms, and critical micelle concentrations can be estimated if an appropriate database is accessible. For example, surfactant surface tension or adsorption data are predictable from known data of homologous surfactants following Traube's rule[119] that states the regular variation of properties with the number of methylene groups, N_{CH_2}. Similarly, critical micelle concentrations for homologous compounds have been correlated with N_{CH_2}.[119,120] Further, the system of Giles, which classifies surfactants according to the similarity between the shapes of their adsorption isotherms, can provide information about the adsorption mechanism.[121] In general, however, we caution against the use of similarity arguments to promote the mechanistic understanding of molecular behavior, unless jointly applied within the framework of theoretical and simulation techniques. Nevertheless, the rapid growth of chemical data urges the need for knowledge-based filtering of information according to a task at hand, and here similarity methods offer substantial support.

Film Similarity. Organic monolayer films can be formed by the adsorption of amphiphilic molecules on a solid substrate. Films that are built by spontaneous organization of amphiphilic molecules into dense quasi-crystalline or liquid structures are called self-assembled monolayers (SAM).[122] Typically, SAMs are prepared by immersion of planar metallic films, for example an Au(111) film grown epitaxially on mica, in a tenside solution under controlled conditions. In contrast, conditions in TSP systems often change, and the composition, size, and surface structure of the particles may not be resolved. Comparison of TSP with SAM systems should provide valuable clues with respect to film structure, stability, and phase behavior. Similarity searches through the rich SAM-literature needs some effort; automatic searches that were encouraged for molecular information are limited due to the lack of a standard format for film and nanosystem data. Monolayer similarities may directly be studied for model systems using computer simulations that provide a powerful approach to evaluate important features, rules, and trends for similar monolayers. For instance, geometric properties, order parameters, and density profiles have been presented as a function of amphiphile density and amphiphile chain length by cubic lattice MC-simulation for athermal nanosystems.[76] These studies have been extended to branched amphiphiles,[78] to analogous amphiphiles with differently structured head groups,[77] and to mixtures of homologous amphiphiles.[85] The self-adjusted surface coverage of a film with amphiphiles that may detach themselves from the surface has been studied as a function of amphiphile length and head-group energies within the cubic lattice model[123] and within the bond-fluctuation model[82] confirming the experimental observation that short amphiphiles tend to replace their longer homologues.[124]

Surface Similarity. The atomic topography of a solid surface can be described by application of scanning tunneling microscopy,[125] requiring prepared substrates. Although not directly applicable to TSPs, surface data derived from STM studies may have information in storage for predicting the topography of the surface of process particles assuming similar material properties for the prepared substrate and the TSPs. However, description of surface energetics and interaction with adjacent bulk phases and adsorbed molecules has to account for chemical heterogeneity and roughness of the particles. Instead of deriving particle surface models from scanned images of surfaces, we decided to apply deposition models to generate model surfaces in the cubic lattice. In the following, the ballistic deposition, BD, model, the diffusion deposition, DD, model, and the model for corrugated surfaces, CO, will be introduced to generate chemically homogeneous surfaces with quantified roughness

to be used in subsequent monolayer simulations. Deposition models are usually explained in terms of sinking particles eventually arriving at a site they will occupy permanently. It should be noted that the particles in the deposition models do not resemble TSPs. In fact, the deposition particles in the next paragraph do not have any physical meaning at all; they merely serve the purpose of generating model surfaces.

THE SURFACE MODELS

BD Model. We have applied the BD model[93,126,127] to generate model surfaces in a lattice cuboid **C** of size $L_x \cdot L_y \cdot L_z$. ***C****(x, y, z)* is a defined lattice site of the cuboid while $0 \le x < L_x$, $0 \le y < L_y$, and $0 \le z < L_z$. Periodic boundary conditions apply in *x*- and *y*-directions. Starting with a cuboid of empty lattice sites, a surface is built from particles whereby each of the particles occupy one lattice site. A particle is generated in a random (*x, y*)-column at the ceiling of the cuboid ($z = L_z - 1$). Thereafter, the particle moves downward in this column and will come to rest either at **C**(*x, y,* 0) or at the first site that has an occupied site located underneath or at a laterally adjacent site. The newly occupied site becomes a surface site. The layer position *z* of this surface site defines the surface height *h(x, y)* for the (*x, y*)-column. Deposition of new particles is continued by the same procedure until a surface of desired root-mean-square roughness R_{rms} will be obtained[129]

$$R_{rms} \equiv \sqrt{\frac{1}{N_{col}} \sum_{x=1}^{L_x} \sum_{y=1}^{L_y} [h(x, y) - \bar{h}]^2}$$

where N_{col} equals the number of (*x, y*)-columns, $L_x \cdot L_y$, and $\bar{h}$ is the mean of the surface heights *h(i, j)*. This definition is independent of the surface generation model and will further be used for DD- and CO-surfaces introduced below.

Any lattice site not being a surface site itself but having at least one adjacent surface site is denoted as a contact site. We distinguish between ceiling, bottom, and steep contact sites. **C**(*x, y, z*) is a ceiling contact site if **C**(*x, y, z*+1) is a surface site. **C**(*x, y, z*) is a bottom contact site if it is not a ceiling contact site and if **C**(*x, y, z*−1) is a surface site. Contact sites that do not fall in either of these categories are steep contact sites. We call a surface that contains at least one ceiling contact site a concave lattice surface. Otherwise, we call the lattice surface convex. Concave lattice surfaces are models for nanoporous surfaces. A concave lattice surface is turned into a convex lattice surface by filling the concavities with surface particles, i.e. by placing particles on each unoccupied **C**(*x, y, z*) with $0 \le z < h(x, y)$. Applying this procedure, both the concave BD-surface, B_{cav}, and the convex BD-surface, B_{vex}, have the same R_{rms} values. Figure l (parts a and b) shows cross sections of a Bcav and a corresponding Bvex surface. For this study, we have generated Bcav and Bvex surfaces with $R_{rms} = 1.30$, 2.17, and 2.82.

DD-Model. The DD-model is a modified random deposition, RD, model.[128] In the RD-model particles simply sink down onto the surface. In the DD-model, a particle deposited in a random (*x, y*)-column is allowed to diffuse into one of the four nearest-neighbor columns. Finally, the particle will stick to the top of the solid column (*x, y*), (*x*+1, *y*), (*x*−1, *y*), (*x, y*+1), or (*x, y*−1), depending on which column offers the deepest sticking site. If the deepest-sticking rule is satisfied by more than one column, random selection applies. Periodic boundary conditions are observed. A cross section of a typical DD-surface is shown in Figure 1c. In contrast to the BD-model, the DD-model always generates convex surfaces with "smooth roughness". This is illustrated in Figure 2 where the roughness of BD- and DD-surfaces are compared. Surface roughness is shown against the deposition time equal to $t \cdot L_x \cdot L_y$ deposited particles. Clearly, the BD-model allows for much rougher surfaces than the DD-model. For $t > 10$ the DD-model generates nearly equally rough surfaces independent of *t*. DD-surfaces with R_{rms} values between 0.4 and 0.7 have been generated for this study.

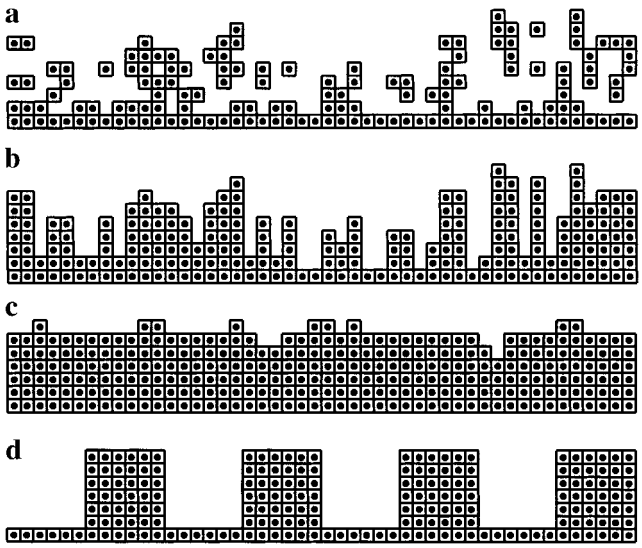

Figure 1. Cross section through model surfaces: (a) Bcav-surface, (b) Bvex-surface, (c) DD-surface, and (d) CO-surface.

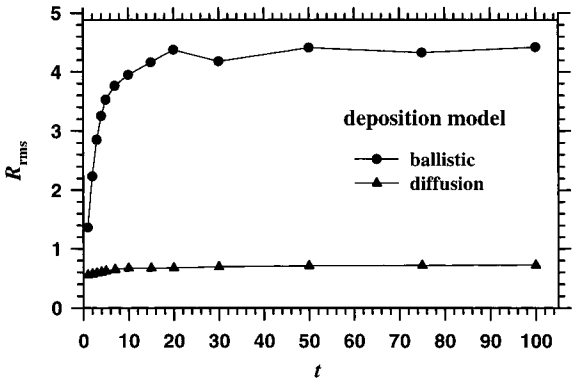

Figure 2. Comparison of the surface roughness for surfaces generated with the ballistic and the diffusion deposition model.

CO Model. Rough, corrugated surfaces have been applied in a MC-study of the adsorption of triblock copolymers.[87] Given a planar surface of size $L_x \cdot L_y$, a corrugated surface is generated by aligning columns of height L_y and with a square base of area $L_{CO} \cdot L_{CO}$ on this surface in such a way that the distance between the walls of two neighbor columns is L_{CO}. Figure 1d shows a cross section of a CO-surface with $L_{CO} = 6$. If Mod[2 L_{CO}, L_x] = 0, then the equation $R_{rms} = \bar{h} = {}^1/_2 L_{CO}$ holds for CO-surfaces. We will study surfaces with $L_{CO} = 1$, 2, 3, 4, and 6.

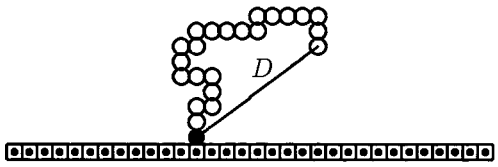

Figure 3. Arbitrary conformation of an amphiphilc chain with end−end distance D grafted onto a planar surface.

Monte Carlo Simulation of Single Chains and Monolayers. Surfactants tend to exhibit some solubility in aqueous solution and some affinity for lipophilic solvents. This ambivalent character is modeled by dividing surfactant molecules into distinct submolecular groups. In our study, an amphiphilic molecule consists of M groups, also called segments. The first segment is a hydrophilic head group followed by $M-1$ hydrophobic tail segments. Two successive segments along the chain occupy a pair of adjacent lattice sites. Figure 3 shows a 2D-chain grafted with its head segment onto a planar surface. MC-simulation of the chain behavior requires repeated growth of chain molecules being achieved with the restricted random walk, RRW, and the self-avoiding walk, SAW, algorithm.[17,130] Both approaches are subjected to the excluded-volume interaction ensuring that chains do not intersect with themselves, with each other, or with the surface. The RRW algorithm differs from the SAW approach in the sampling mode. The RRW algorithm selects the site for a successive segment randomly from the four (2D) or six (3D) nearest-neighbor sites irrespective of their status of occupation, whereas the SAW algorithm performs biased sampling[14] that selects the successive site randomly from the set of unoccupied nearest neighbor sites. Chain growth with the RRW algorithm terminates as soon as an occupied site is selected, thus, allowing for unbiased chain sampling. However, compilation of a statistically satisfying number of sample chains requires a huge number of growth trials increasing rapidly with chain length. Therefore, in monolayer simulations the SAW algorithm is applied to enhance chain growth efficiency. With the SAW algorithm, chain growth is only terminated in case of a deadend, i.e. if all nearest neighbor sites are occupied. For long chains the probability of running into a deadend increases exponentially with M. This severe limitation in sampling long chain conformations is known as the attrition problem.[14,17] We will demonstrate the attrition problem for 2D-chains in bulk space and on a planar surface.

We represent a TSP system through a canonical or *NVT* ensemble with a fixed number of molecules N placed in a cuboid of fixed volume $V = L_x \cdot L_y \cdot L_z$ at constant temperature T. We perform athermal simulations applying excluded volume interactions but neither attractive nor repulsive interactions ($T = \infty$). Head segments of the chains are confined to contact sites, whereas tail segments are allowed on any nonsurface site inside the cuboid. A contact site occupied by a head segment is denoted as grafting site. Chain moves during MC-simulation always begin with a random selection of a new grafting site in the neighborhood including the current grafting site. Then, an attempt is made to grow a new SAW-chain from the new head position. To counterbalance the preferential growth of certain chain conformations due to the bias of SAW sampling, we introduce the ratio of the Rosenbluth weights,[15] W_{trial}/W_{cur}, where W_{trial} and W_{cur} are the weights for the trial and for the current conformation, respectively. An attempted move is accepted with probability $P = \min(1, W_{trial}/W_{cur})$. The realization of N accepted conformations is named a MC-step.

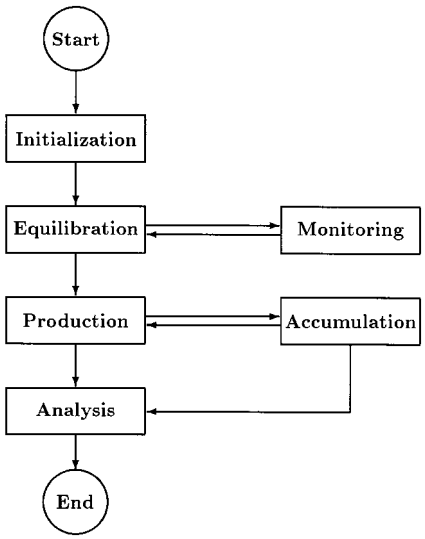

Figure 4. Flow chart for a Monte Carlo simulation run.

As illustrated in Figure 4, a particular run of a MC-simulation includes an equilibration and production procedure followed by analysis of data accumulated through production. Initial monolayers with head densities $\Phi = N/(L_x \cdot L_y)$ were constructed with straight chains perpendicular to the x,y-plane. We relaxed the initial monolayer configuration during 10^6 MC-steps, while advancement of the equilibrium conditions was monitored. Then, production followed with $2 \cdot 10^5$ MC-steps. During production, we secured $K = 100$ ensemble configurations equidistantly separated by 10^3 MC-steps for detailed analyses after completion of the MC-procedure. Ensemble configurations were analyzed with respect to SSC-probabilities, grafting densities, and mean geometrical properties.

SSC-Probabilities. Segments in a chain are enumerated from $j = 1$ to $j = M$, with $j = 1$ being the head segment and $j = 2$ being the α-segment. A segment has surface contact if and only if it occupies a contact site. The SSC-probability of the jth segment is defined as

$$P_{SSC}(j) = \frac{1}{KN}\sum_{k=1}^{K} S_i(j)$$

where $S_i(j) = 1$ if the jth segment of the ith molecule in the monolayer has surface contact, otherwise $S_i(j) = 0$. Summation is done over all secured ensemble configurations.

Mean Geometric Properties. Mean geometric properties are derived from the molecular end−end vector,[76] which is determined by the site of the head segment $\mathbf{C}(x_H, y_H, z_H)$ and the terminal tail segment $\mathbf{C}(x_T, y_T, z_T)$. We will calculate the relative mean distance between the end segments that is defined as

$$\langle rD \rangle \equiv \frac{1}{K(M-1)}\sum_{k=1}^{K}\left\{\frac{1}{N}\sum_{i=1}^{N}((\Delta x_{i,k})^2 + (\Delta y_{i,k})^2 + (\Delta z_{i,k})^2)\right\}^{1/2}$$

where $\Delta x = x_T - x_H$, $\Delta y = y_T - y_H$, and $\Delta z = z_T - z_H$.

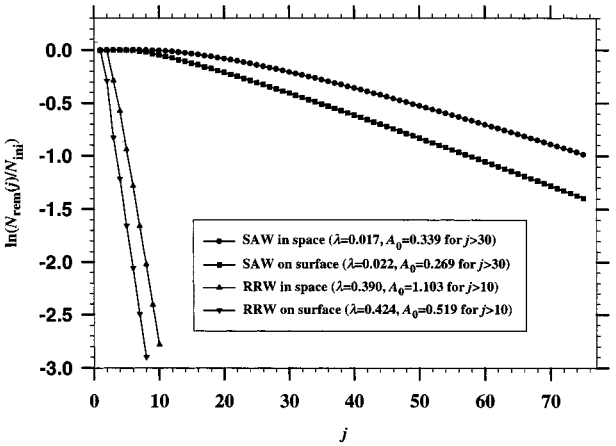

Figure 5. Attrition problem for SAW and RRW chains growing in space and on a planar surface (λ an A_0 were obtained by linear regression, consult text).

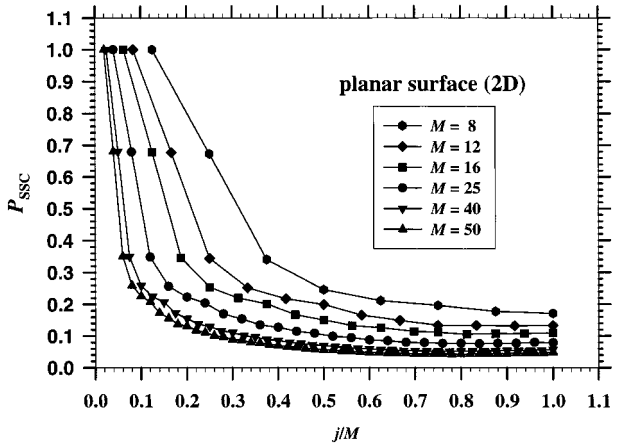

Figure 6. Segment−surface contact probabilities vs normalized segment positions for two-dimensional chains of different length on a planar surface.

Mean Grafting Density. Grafting sites[93] are analyzed in dependence on the height $h(x,y)$ of the surface column located underneath the grafting site. We define the mean grafting density

$$\langle \varphi_G(h) \rangle \equiv \frac{1}{K} \sum_{k=1}^{K} \frac{N_{G,k}(h)}{N_{col}(h)}$$

where $N_{G,p}(h)$ is the number of grafting sites above a surface column of height h at snapshot k and $N_{col}(h)$ is the number of surface columns of height h.

RESULTS AND DISCUSSION

I. Single Two-Dimensional Chains. Attrition Problem. We have generated 2D-chains with a maximum of 75 segments employing both the RRW and the SAW algorithm. At least $N_{ini} = 10^6$ chains were initialized to grow, while the number of remaining chains with j segments, $N_{rem}(j)$, are registered. Chains remain as long as self-avoidance with respect to the particular growth algorithm is obeyed. We did four runs: RRW in space, RRW on surface, SAW in space, and SAW on surface. For each run, $\ln(N_{rem}(j)/N_{ini})$ against j is plotted in Figure 5. The probability of successfully generating chains above 10 segments with the RRW algorithm decreases dramatically. The situation is appreciably better for SAW chains. Irrespective of the growth algorithm, growth in space has a larger success rate than growth on a surface. The straight part of the curves can be presented by the following correlation equation

$$\ln\left(\frac{N_{rem}}{N_{ini}}\right) = A_0 - \lambda \cdot j$$

where A_0 and λ are regression coefficients. The coefficient λ is called the attrition constant. Regression results are displayed in Figure 5 where the correlation coefficient r^2 is greater than 0.998 in all cases. Our "RRW in space" case is identical with the "4-choice 90°" case in the literature,[17] and our λ value of 0.390 agrees well with the corresponding literature value of 0.408. The attrition constant is a parameter being specific for a particular growth algorithm, lattice type, and surface environment. It measures the efficiency of a growth algorithm for its application in MC-simulations. Our results underline that the attrition problem has a larger impact for chain growth on a surface than for isotropic growth. Our studies of single chain attrition provide a best-case scenario. For monolayer simulations, the attrition problem increases with increasing density of chains in the layer. We were carefully monitoring chain attrition and growth success during our monolayer simulations to ensure statistically meaningful sampling of the configuration space.

SSC-Probability. For six different chain lengths, we have sampled at least 10^6 conformations grown with the SAW algorithm on a planar surface. In Figure 6, P_{SSC} is plotted against the normalized segment position j/M. With the exclusion of chains with $M = 8$, the SSC-probability always decreases toward a minimum at about $j_{min} = 0.8M$. Beyond this minimum a very slight increase in P_{SSC} can be observed. For homologues with $M > 40$, similarly shaped and nearly collapsing curves were obtained suggesting identical SSC behavior of linear chains if scaled with respect to chain length.

II. Grafted Three-Dimensional Chains. Athermal MC-simulations have been performed on planar and on rough Bvex-, Bcav-, DD-, and CO-surfaces for monolayers including chains with $M = 8$ and 16 while $\Phi = 0.25$.

SSC-Probability. The SSC-probabilities for chains with 16 segments on a planar and on three Bcav-surfaces are shown in Figure 7. The head density is $\Phi = 0.25$. For all surfaces, the SSC-probability of the α-segment, $P_{SSC}(2)$, is higher than $P_{SSC}(j)$ of the following segments with $j > 2$, for which P_{SSC} decreases until a minimum is reached at about $j_{min} = {}^3/_4M$. $P_{SSC}(2)$ of the α-segments on rough surfaces is smaller than $P_{SSC}(2)$ on the planar surface. For segments with $j > 2$, $P_{SSC}(j)$ on rough surfaces always surpasses the corresponding $P_{SSC}(j)$ on the planar surface. Except for α-segments, $P_{SSC}(j)$ increases significantly with increasing surface roughness. We will refer to the latter trend as the roughness-increases-contacts, RIC, rule. We have repeated these simulations with the same parameters but on Bvex-surfaces. The results are presented in Figure 8 including again the curve for the planar surface. The curves for the rough surfaces look similar in shape to the curves of Figure 7. Most patterns, such as the RIC-rule and the α-segment specialities, are preserved. However, the trend expressed

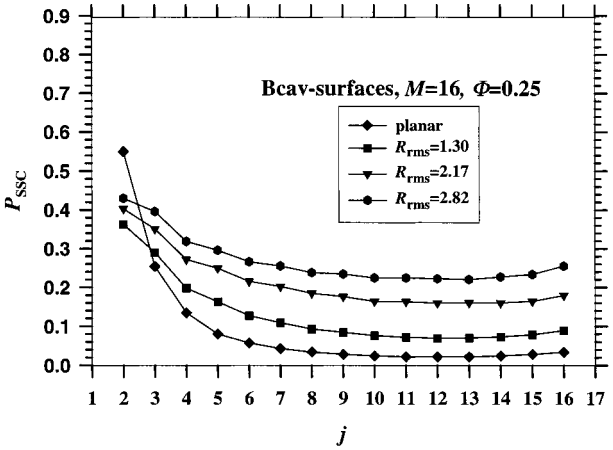

Figure 7. Segment−surface contact probabilities vs segment positions for chains on convex surfaces.

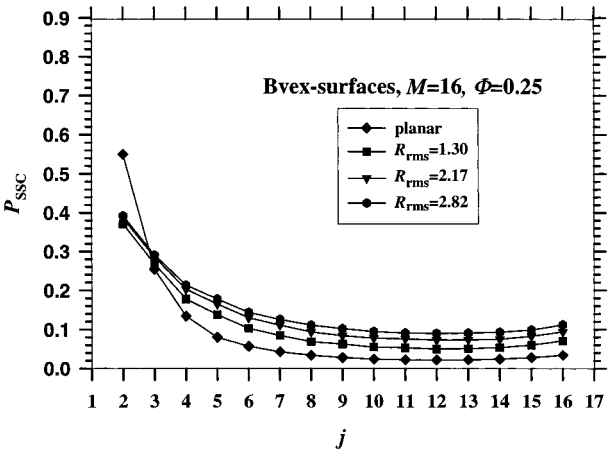

Figure 8. Segment−surface contact probabilities vs segment positions for chains on concave surfaces.

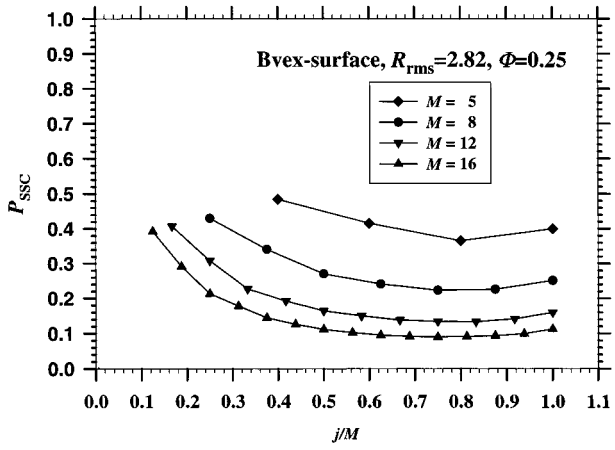

Figure 9. Segment−surface contact probabilities vs normalized segment positions for chains of different length on a convex surface.

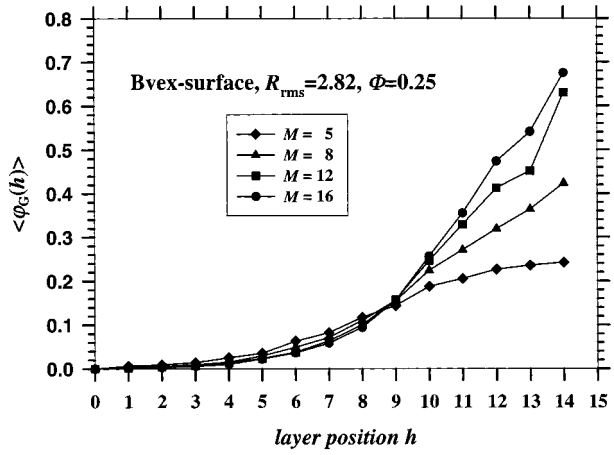

Figure 10. Mean grafting density $\langle\Phi_G\rangle$ vs height h of the surface columns for four different chain lengths.

by the RIC-rule is diminished. The missing cavities decrease the number of contact sites on convex surfaces and thus decrease the chance of segment-surface contacts. Simulation on convex DD-surfaces with R_{rms} values much smaller than the R_{rms} values of the Bvex-simulations show that the curves for higher j collapse with the curve for the planar surface. Again the α-segment specialities are preserved, and a minimum at $j_{min} = {}^3/_4M$ is found. Finally, we repeated the simulations with CO-surfaces. Again, for segments with $j > 2$, $P_{SSC}(j)$ decreases until a minimum is reached at about $j_{min} = {}^3/_4M$. The curve for the surface with the lowest roughness ($L_{CO} = 1$, $R_{rms} = 0.5$) collapses with the curve for the planar surface for $j > 3$. The pattern observed for chains with $M = 16$ were similarly observed in our simulations with chains of length $M = 8$ employing the same head density and the same Bcav-, Bvex-, and CO-surfaces. Further, we did simulation with the same parameters but taking chains of length $M = 5$ and 18. In Figure 9, P_{SSC} is plotted against the normalized length j/M for simulations of chains with 5, 8, 12, and 16 segments at $\Phi = 0.25$ on a Bvex-surface with $R_{rms} = 2.82$. This plot demonstrates again that grafted chains at athermal conditions possess a P_{SSC} minimum at $j_{min} = {}^3/_4M$.

Mean Grafting Density. Figure 10 shows the mean grafting density $\langle\varphi_G(h)\rangle$ for chains with 5, 8, 12, and 16 segments and $\Phi = 0.25$ on a Bvex-surface with $R_{rms} = 2.82$. The maximum surface column height for this surface is 14. For layer positions below height 9, the grafting density of short chains is higher than the grafting density of long chains. Above height 9, this order is reversed: the probability for a long chain to graft at this height is significantly higher than the probability for a short chain. Also at about height 9, inflection occurs for the curve of 5-mers. As a general trend, amphiphiles of any chain length prefer grafting on higher columns. This rule is most pronounced for long chains for which the self- and surface-avoidance is better realized at top positions. Including recent results,[93] we conclude that for a homologous series the tendency of grafting at high surface columns increases with increasing overall head density Φ and with increasing chain length.

Mean Geometrical Properties. Figure 11 shows the relative mean end−end distance $\langle rD\rangle$ versus surface roughness for the simulation of chains with $M = 8$ and $\Phi = 0.25$. The $\langle rD\rangle$ values are reproduceable within ±0.001. The value of 0.517 for the planar surface lies agreably between the previously found values for chains with $M = 5$ and 10 at the same head density.[76] The $\langle rD\rangle$ values for the DD-surfaces are approximately constant and equal to the value for the planar surface suggesting that a small surface roughness does not significantly effect the mean molecular geometry. For Bcav- and Bvex-surfaces the $\langle rD\rangle$ values decrease with increasing roughness. The comparison of concave and convex surfaces shows that the R_{rms} value for the Bcav-surface is always below the Bvex-surface of the

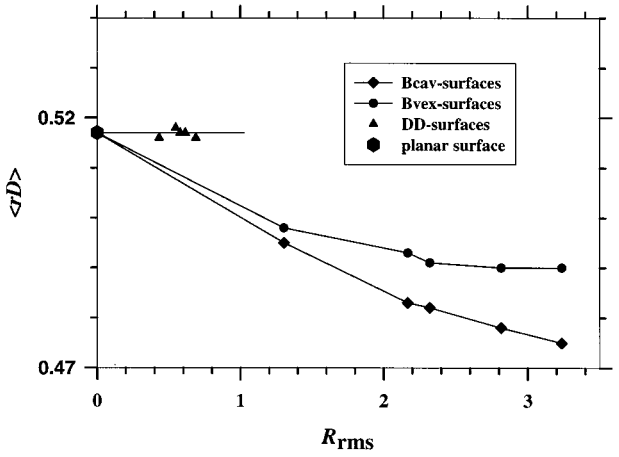

Figure 11. Relative mean end−end distance ($M = 8$, $\Phi = 0.25$) vs surface roughness for different surface topography.

same R_{rms} roughness. One may argue that the switch from a convex to the concave surface parallels a switch to lower head density due to the increase of contact sites. Then, the observed decrease agrees with the similarly observed decrease of $\langle rD \rangle$ values with decreasing head densities on planar[76] and on convex[93] surfaces. However, the effect of surface topography and roughness on $\langle rD \rangle$, with values between 0.47 and 0.52 in Figure 11, is relatively small compared to $\langle rD \rangle$ changes of more than 0.1 going from high to low head density.[76]

Universal Parameters. The reported simulation results are based on a coarse-grained, athermal model where atomistic-level molecular details have been neglected. Instead, a hyperatomic, constrained molecule representation was used to derive properties applying globally for a large set of nanosystems. Most significant, we found a universal chain-surface contact behavior for all investigated systems. Nanosystems related through a universal parameter build a class of similar systems. Often, characteristic scaling laws can be derived for such classes as has been demonstrated for polymer systems.[131] Universal parameters are highly valued for the compression of information and for the efficient prediction of various properties. Property prediction for a particular nanosystem will typically start with the universal, similarity-based approach before advancing toward a detailed, atomistic-level analysis.

CONCLUSIONS

The properties of nanosystems such as the TSP system are required to optimize separation processes. Comparison of TSP systems to similar but less complex systems supports the assessment of TSP properties based on similarity arguments. Further, MC-simulations enabled us to study TSP properties in relation to systematic changes of the structure of the tenside molecules, of the film density, and of the surface properties.

Cubic lattice MC-simulations of adsorbed monolayers reveal similarities and dissimilarities of the segment-surface contact behavior and the geometric properties of grafted surfactant molecules in different nanosystems. In particular, the contact probability for the segments of chains with length M exhibit a minimum at about $^3/_4M$, which is independent of the actual chain length, the head density, and the roughness and topography of the surface. Comparison of individual chain segments shows that the contact probability for α-segments depends on the surface topography. However, the contact probability for the α-segment is always greater than the contact probability for the following chain segments. The relative mean end-end distance is a function of both surface roughness and surface topography. These results have been found with a coarse-grained segment-surface model for athermal conditions. Future work has to include segment−segment, segment−solvent, segment−surface, and solvent−surface interaction terms to build a refined and more realistic model for TSP systems and to account for more chemical diversity among the functional head and tail segments.

The current approach allows the design of model systems with desired surface roughness and topography. MC-initialization of these models requires as input solely design parameters. Without input of empirical data, certain rules of system behavior are derived. These rules will serve as a baseline for the comparison of more refined models and of experimental nanosystem data.

ACKNOWLEDGMENT

This work was supported by funding from the *Deutsche Forschungsgemeinschaft* through the Grant SFB 285 "Particle Technology". We further acknowledge financial support from the *Fonds der Chemischen Industrie.*

REFERENCES AND NOTES

(1) Crandall, B. C.; Lewis, J. *Nanotechnology Research and Perspectives*; The MIT Press: Cambridge, Massachusetts, 1992.
(2) Reid, R. C.; Praussnitz, J. M.; Poling, B. E. *The Properties of Gases and Liquids*; 4th ed.; McGraw-Hill Book Company: Singapore, 1988.
(3) van Krevelen, D. W. *Properties of Polymers*, 3rd ed.; Elsevier Science Publishing Company: Amsterdam, 1990.
(4) Horvath, A. L. *Molecular Design*; Elsevier: Amsterdam, 1992.
(5) Lyman, W. J.; Reehl, W. F.; Rosenblatt, D. H. *Handbook of Chemical Property Estimation Methods*; American Chemical Society: Washington, DC, 1990.
(6) *Physical Property Prediction in Organic Chemistry*; Jochum, C., Hicks, M. G., Sunkel, J., Eds.; Springer-Verlag: Berlin, 1988.
(7) Drefahl, A.; Reinhard, M. *Handbook for Estimating Physico-Chemical Properties of Organic Compounds*; Stanford Bookstore: Stanford, CA 94305, 1995.
(8) Israelachvili, J. N. *Intermolecular and Surface Forces*; 2nd ed.; Academic Press: London, 1992.
(9) Haile, J. M. *Molecular Dynamics Simulation*; John Wiley & Sons, Inc.: New York, 1992.
(10) Allen, M. P.; Tildesley, D. J. *Computer Simulation of Liquids*; Clarendon Press: Oxford, 1996.
(11) *Monte Carlo and Molecular Dynamics Simulations in Polymer Science*; Binder, K., Ed.; Oxford University Press: New York, 1995. (a) Clarke, J. H. R. Chapter 5 therein.
(12) Allen, M. P.; Tildesley, D. J. *Computer Simulation in Chemical Physics*; Kluwer Academic Publishers: Dordrecht, 1993.
(13) *The Monte Carlo Method in Condensed Matter Physics*; Binder, K., Ed.; Springer-Verlag: Berlin 1992.
(14) Binder, K.; Heermann, D. W. *Monte Carlo Simulation in Statistical Physics*; Springer-Verlag: 1992.
(15) Rosenbluth, M. N.; Rosenbluth, A. W. Monte Carlo Calculation of the Average Extension of Molecular Chains. *J. Chem. Phys.* **1955**, *23*, 356−359.
(16) Wall, F. T.; Hiller, L. A.; Wheeler, D. J. Statistical Computation of Mean Dimension of Macromolecules. I. *J. Chem. Phys.* **1954**, *22*, 1036−1041.
(17) Wall, F. T.; Hiller, L. A.; Atchison, W. F. Statistical Computation of Mean Dimension of Macromolecules. II. *J. Chem. Phys.* **1955**, *23*, 913−921.
(18) Wall, F. T.; Hiller, L. A.; Atchison, W. F. Statistical Computation of Mean Dimension of Macromolecules. III. *J. Chem. Phys.* **1955**, *23*, 2314−2321.

(19) Wall, F. T.; Hiller, L. A.; Atchison, W. F. Statistical Computation of Mean Dimension of Macromolecules. IV. *J. Chem. Phys.* **1957**, *26*, 1742−1749.
(20) Wall, F. T.; Rubin, R. J.; Isaacson, L. M. Improved Statistical Method for Computing Mean Dimensions of Polymer Molecules. *J. Chem. Phys.* **1957**, *27*, 186−188.
(21) Wall, F. T.; Erpenbeck, J. J. New Method for the Statistical Computation of Polymer Dimensions. *J. Chem. Phys.* **1959**, *30*, 634−637.
(22) Wall, F. T.; Erpenbeck, J. J. Statistical Computation of Radii of Gyration and Mean Internal Dimension of Polymer Molecules. *J. Chem. Phys.* **1959**, *30*, 637−640.
(23) Wall, F. T.; Mandel, F. Monte Carlo of Chains with Excluded Volume: Distribution of Intersegmental Distances. *J. Chem. Phys.* **1975**, *54*, 5338−5345.
(24) Alexandrowicz, Z.; Accad, Y. *J. Chem. Phys.* **54** (1971) 5338.
(25) Verdier, P. H.; Stockmayer, W. H. Monte Carlo Calculations on the Dynamics of Polymers in Dilute Solution. *J. Chem. Phys.* **1962**, *36*, 227−235.
(26) Verdier, P. H. Monte Carlo Studies of Lattice-Model Polymer Chains. II. End-to-End Length. *J. Chem. Phys.* **1966**, *45*, 2122−2128.
(27) Baumgärtner, A.; Binder, K. Monte Carlo studies on the freely jointed polymer chain with excluded volume interaction. *J. Chem. Phys.* **1979**, *71*, 2541−2545.
(28) Baumgärtner, A. Statics and dynamics of the freely jointed polymer chain with Lennard−Jones interaction. *J. Chem. Phys.* **1980**, *72*, 871−879.
(29) Nunes, N. L.; Chen, K.; Hutchinson, J. S. Flexible Lattice Model To Study Protein Folding. *J. Chem. Phys.* **1996**, *100*, 10443−10449.
(30) Sheng, Y.-J.; Panagiotopoulos, A. Z.; Kumar, S. K.; Szleifer, I. Monte Carlo Calculation of Phase Equilibria for a Bead-Spring Polymeric Model. *Macromolecules* **1994**, *27*, 400−406.
(31) Haliloglu, T.; Balaji, R.; Mattice, W. L. Mobility of Free Ends and Junction Points in a Lamellar Block Copolymer. *Macromolecules* **1994**, *27*, 1473−1476.
(32) Downey, J. P. Static and Dynamic Scaling Properties of Single, Self-Avoiding Polymer Chains in Two Dimensions via the Bond Fluctuation Method of Monte Carlo Simulation. *Macromolecules* **1994**, *27*, 2929−2932.
(33) Mansfield, M. L. Concentrated, Semiflexible Lattice Chain Systems and Criticism of the Scanning Technique. *Macromolecules* **1994**, *27*, 4699−4704.
(34) Fawcett, A. H.; Mee, R. A. W.; McBride, F. V. A Monte-Carlo Study of Ring Formation and Molecular Configurations during Step Growth on a Lattice in Three Dimensions. *Macromolecules* **1995**, *28*, 1481−1490.
(35) Rubio, A. M.; Freire, J. J.; Bishop, M.; Clarke, J. H. R. Φ State, Transition Curves, and Conformational Properties of Cyclic Chains. *Macromolecules* **1995**, *28*, 2240−2246.
(36) Nguyen-Misra, M.; Mattice, W. L. Dynamics of End-Associated Triblock Copolymer Networks. *Macromolecules* **1995**, *28*, 6976−6985.
(37) Rapold, R. F.; Mattice, W. L. Introduction of Short and Long Range Energies To Simulate Real Chains on the *2nnd* Lattice. *Macromolecules* **1996**, *29*, 2457−2466.
(38) Barenbrug, Th. M. A. O. M.; Smit, J. A. M.; Bedeaux, D. Conformational Free Energy of Lattice Polyelectrolytes with Fixed Endpoints. I. Single-Chain Simulation and Theory. *Macromolecules* **1997**, *30*, 605−619.
(39) Baschnagel, J.; Binder, K.; Paul, W.; Laso, M.; Suter, U. W.; Batoulis, I.; Jilge, W.; Bürger, T. On the construction of coarse-grained models for linear flexible polymer chains: Distribution functions for groups of consecutive monomers. *J. Chem. Phys.* **1991**, *95*, 6014−6025.
(40) Yethiraj, A.; Dickman, R. Local structure of model polymeric fluids: Hard-sphere chains and the three-dimensional fluctuating bond model. *J. Chem. Phys.* **1992**, *97*, 4468−4475.
(41) Geroff, I.; Milchev, A.; Binder, K.; Paul, W. A new off-lattice Monte Carlo model for polymers: A comparison of static and dynamic properties with the bond-fluctuation model and application to random media. *J. Chem. Phys.* **1993**, *98*, 6526−6539.
(42) Rodriguez, A. L.; Wittmann, H.-P.; Binder, K. Orientational Ordering in Two-Dimensional Polymer Solutions: Monte Carlo Simulations of a Bond Fluctuation Model. *Macromolecules* **1990**, *23*, 4327−4335.
(43) Molina, L. A.; Freire, J. J. Monte Carlo Study of Symmetric Diblock Copolymers in Selective Solvents. *Macromolecules* **1995**, *28*, 2705−2713.
(44) Irvine, D. J.; Gersappe, D.; Balazs, A. C. Computer Simulations of Self-Assembling Comb Copolymers. *Langmuir* **1995**, *11*, 3848−3855.
(45) Ko, M. B.; Mattice, W. L. Monte Carlo Simulation of Concentrated Diblock Copolymers in a Selective Solvent: Anisotropy of the Diffusion. *Macromolecules* **1995**, *28*, 6871−6877.
(46) Bruns, W. The Second Osmotic Virial Coefficient of Polymer Solutions. *Macromolecules* **1996**, *29*, 2641−2643.
(47) Xing, L.; Mattice, W. I. Strong Solubilization of Small Molecules by Triblock-Copolymer Micelles in Selective Solvents. *Macromolecules* **1997**, *30*, 1711−1717.
(48) Sariban, A.; Binder, K. Critical properties of the Flory-Huggins lattice model of polymer mixtures. *J. Chem. Phys.* **1987**, *86*, 5859−5873.
(49) Deutsch, H. P.; Binder, K. Interdiffusion and self-diffusion in polymer mixtures: A Monte Carlo study. *J. Chem. Phys.* **1991**, *94*, 2294−2304.
(50) Gunn, J. R.; Dawson, K. A. A lattice model description of amphiphilic mixtures. I. Equilibrium properties. *J. Chem. Phys.* **1992**, *96*, 3152−3169.
(51)) Müller, M.; Binder, K. Computer Simulation of Asymmetric Polymer Mixtures. *Macromolecules* **1995**, *28*, 1825−1834.
(52) Ypma, G. J. A.; Cifra, P.; Nies, E.; van Bergen, A. R. D. Interfacial Behavior of Compressible Polymer Blends. Monte Carlo Simulation and the Lattice Fluid Theory. *Macromolecules* **1996**, *29*, 1252−1259.
(53) Cifra, P.; Nies, E.; Broersma, J. Equation of State and Miscibility Behavior of Compressible Binary Lattice Polymers. A Monte Carlo Study and Comparison with Partition Function Theories. *Macromolecules* **1996**, *29*, 6634−6644.
(54) Dadmun, M. Effect of Copolymer Architecture on the Interfacial Structure and Miscibility of a Ternary Polymer Blend Containing a Copolymer and Two Homopolymers. *Macromolecules* **1996**, *29*, 3868−3874.
(55) Baumgdirtner, A. Glass transition of a polymer chain. *J. Chem. Phys.* **1980**, *73*, 2489−2494.
(56) Baumgartner, A.; Binder, K. Dynamics of entangled polymer melts: A computer simulation. *J. Chem. Phys.* **1981**, *75*, 2994−3005.
(57) Meirovitch, H. Efficient Dynamical Monte Carlo Method for Dense Polymer Systems. *Macromolecules* **1984**, *17*, 2038−2044.
(58) Paul, W.; Pistoor, N. A Mapping of Realistic onto Abstract Polymer Models and an Application to Two Bisphenol Polycarbonates. *Macromolecules* **1994**, *27*, 1249−1255.
(59) Larson, R. G. Simulation of Lamellar Phase Transitions in Block Copolymers. *Macromolecules* **1994**, *27*, 4198−4203.
(60) Pant, P. V. K.; Theodorou, D. N. Variable Connectivity Method for the Atomistic Monte Carlo Simulation of Polydisperse Polymer Melts. *Macromolecules* **1995**, *28*, 7224−7234.
(61)) Freire, J. J.; Prats, R.; Pla, J.; de la Torre, J. G. Hydrodynamic Properties of Flexible Branched Chains. Monte Carlo Nonpreaveraged Calculations for Stars and Preaveraged Results for Combs. *Macromolecules* **1984**, *17*, 1815−1821.
(62) Romantsova, I.; Taran, Y. Computer simulation of the dynamics of branched polymers. *Makromol. Chem.* **1990**, *191*, 2423−2433.
(63) Gersappe, D.; Fasolka, M.; Israels, R.; Balazs, A. C. Contrasting the Compatibilizing Activity of Comb and Linear Copolymers. *Macromolecules* **1994**, *28*, 720−724.
(64) Vlahos, C. H.; Horta, A.; Hadjichristidis, N.; Freire, J. J. Monte Carlo Calculations of A_xB_{f-x} Miktoarms Star Copolymers. *Macromolecules* **1995**, *28*, 1500−1505.
(65) (65) Ohno, K.; Shida, K.; Kimura, M.; Kawazoe, Y. Monte Carlo Study of the Second Virial Coefficient of Star Polymers in a Good Solvent. *Macromolecules* **1996**, *29*, 2269−2274.
(66) Rouault, Y.; Borisov, O. V. Comb-Branched Polymers: Monte Carlo Simulation and Scaling. *Macromolecules* **1996**, *29*, 2605−2611.
(67) Forni, A.; Ganazzoli, F.; Vacatello, M. Local Conformation of Regular Star Polymers in a Good Solvent: A Monte Carlo Study. *Macromolecules* **1996**, *29*, 2994−2999.
(68) Rubio, A. M.; Freire, J. J. Monte Carlo Calculations of Second Virial Coefficients for Linear and Star Chains in a Good Solvent. *Macromolecules* **29** (1996) 6946−6951.
(69) Chen, Z. Y.; Cui, S.-M. Monte Carlo Simulations of Star-Burst Dendrimers. *Macromolecules* **1996**, *29*, 7943−7952.
(70) Harris, J.; Rice, S. A. A lattice model of a supported monolayer of amphiphile molecules: Monte Carlo simulations. *J. Chem. Phys.* **1988**, *88*, 1298−1306.
(71)) Chakrabarti, A..; Toral, R. Density Profile of Terminally Anchored Polymer Chains: A Monte Carlo Study. *Macromolecules* **1990**, *23*, 2016−2021.
(72) Milik, M.; Kolinski, A.; Skolnick, J. Monte Carlo dynamics of a dense system of chain molecules constrained to lie near an interface. A simplified membrane model. *J. Chem. Phys.* **1990**, *93*, 4440−4446.
(73) Collazo, N.; Rice, S. A. Long-Chain Amphiphile Monolayers on an Anisotropic Substrate: A Computer Simulation Study. *Langmuir* **1991**, *7*, 3144−3153.
(74) Levine, Y. K.; Kolinski, A.; Skolnick, J. Monte Carlo dynamics study of motions in cis-unsaturated hydrocarbon chains. *J. Chem. Phys.* **1991**, *95*, 3826−3834.
(75) Levine, Y. K.; Kolinski, A.; Skolnick, J. A lattice dynamics study of a Langmuir monolayer of monounsaturated fatty acids. *J. Chem. Phys.* **1993**, *98*, 7581−7587.

(76) Stettin, H.; Friedemann, R.; Mögel, H.-J. Monte Carlo Simulations of Supported Monolayers of Amphiphilic Molecules. *Ber. Bunsenges. Phys. Chem.* **1993**, *97*, 44−48.
(77) Stettin, H.; Mögel, H.-J. Amphiphilic molecules with a structured head on a water surface: a Monte Carlo simulation. *Progr. Colloid Polym. Sci.* **1994**, *97*, 27−30.
(78) Stettin, H.; Mögel, H.-J. Branched amphiphilic molecules on a water surface: a Monte Carlo simulation. *Progr. Colloid Polym. Sci.* **1994**, *97*, 31−34.
(79) Gauger, A.; Pakula, T. Static Properties of Noninteracting Comb Polymers in Dense and Dilute Media. A Monte Carlo Study. *Macromolecules* **1995**, *28*, 190−196.
(80) Lai, P.-Y.; Binder, K. Structure and dynamics of grafted polymer layers: A Monte Carlo simulation. *J. Chem. Phys.* **1991**, *95*, 9288−9299.
(81) Lai, P.-Y.; Binder, K. Structure and dynamics of polymer brushes near the Φ point: A Monte Carlo simulation. *J. Chem. Phys.* **1992**, *97*, 586−595.
(82) Lai, P.-Y. Grafted polymer layers with chain exchange: A Monte Carlo simulation. **1993**, *98*, 669−673.
(83) Haas, F. M.; Lai, P.-Y.; Binder, K. Linear chain surfactants at a planar interface: a comparative Monte Carlo study of several lattice models. *Makromol. Chem., Theory Simul.* **1993**, *2*, 889−899.
(84) Kopf, A.; Baschnagel, J.; Wittmer, J.; Binder, K. On the Adsorption Process in Polymer Brushes: A Monte Carlo Study. *Macromolecules* **1996**, *29*, 1433−1441.
(85) Stettin, H.; Wahab, M.; Schiller, P.; Mbgel, H.-J. Self-assembling of chain molecules in low dimensions: a Monte Carlo study. *Makromol. Theory Simul.* **1995**, *4*, 1015−1037.
(86) Stettin, H.; Mögel, H.-J.; Care, C. M. Monolayer Model Simulations of Mixtures of Amphiphilic Molecules. *Ber. Bunsenges. Phys. Chem.* **1996**, *100*, 20−26.
(87) Balazs, A. C.; Huang, K.; Lantman, C. W. Adsorption of Triblock Copolymers on Rough Surfaces. *Macromolecules* **1990**, *23*, 4641−4647.
(88) Gersappe, D.; Fasolka, M.; Israels, R.; Balazs, A. C. Modeling the Behavior of Random Copolymer Brushes. *Macromolecules* **1995**, *28*, 4753−4755.
(89) (89) Clancy, T. C.; Webber, S. E. Pivot Algorithm Computer Simulation of the Effect of Grafted Polymers on the Adsorption of Polymers by a Surface. *Macromolecules* **1995**, *28*, 2561−2569.
(90) Clancy, T. C.; Webber, S. E. Controlling Adsorption of Polymers at Polymer-Modified Surfaces. *Macromolecules* **1997**, *30*, 1340−1346.
(91) Balasubramanian, S.; Klein, M. L.; Siepman, J. I. Monte Carlo investigation of hexadecane films on a metal substrate. *J. Chem. Phys.* **1995**, *103*, 3184−3195.
(92) Wijmans, C. M.; Linse, P. Monte Carlo simulations of the adsorption of amphiphilic oligomers at hydrophobic interfaces. *J. Chem. Phys.* **1997**, *106*, 328−338.
(93) Drefahl, A.; Seidel, O; Mögel, H.-J. *Thin Solid Films*, accepted for publication.
(94) Shaffer, J. S. Monte Carlo Simulations of Random Copolymers near Solid Surfaces. *Macromolecules* **1995**, *28*, 7447−7453.
(95) Misra, S.; Mattice, W. L. Telechelic Polymers between Two Impenetrable Adsorbing Surfaces. *Macromolecules* **1994**, *27*, 2058−2065.
(96) Misra, S.; Nguyen-Misra, M.; Mattice, W. L. Bridging by Reversibly Adsorbed Telechelic Polymers: A Transient "Network". *Macromolecules* **1994**, *27*, 5037−5042.
(97) Nguyen-Misra, M.; Misra, S.; Mattice, W. L. Bridging by End-Adsorbed Triblock Copolymers. *Macromolecules* **1996**, *29*, 1407−1415.
(98) Klein, J.; Kamiyama, Y.; Yoshizawa, H.; Israelachvili, J. N.; Fetters, L. J.; Pincus, P. Modification of Long-Ranged Forces by Surface Exchange of Polymeric Amohiphiles. *Macromolecules* **1992**, *25*, 2062−2064.
(99) Myers, D. *Surfactant Science and Technology;* VCH Publishers, Inc.: Weinheim, 1988.
(100) *Colloid and Surface Engineering: Applications in the Process Industries;* Williams, R. A., Ed.; Butterworth-Heinemann Ltd: Oxford, 1992.
(101) Attia, Y. A. *Colloid separation by selective flocculation;* Chapter 5 in ref 100.
(102) Johnson, M. A.; Maggiora, G. M. *Concepts And Applications of Molecular Similarity;* John Wiley & Sons, Inc.: New York, 1990.
(103) Wild, D. J.; Willett, P. Similarity Searching in Files of Three-Dimensional Chemical Structures. Alignment of Molecular Electrostatic Potential Fields with a Genetic Algorithm. *J. Chem. Inf. Comput. Sci.* **1996**, *36*, 159−167.
(104) Thorner, D. A.; Wild, D. J.; Willett, P.; Wright, P. M. Similarity Searching in Files of Three-Dimensional Chemical Structures: Flexible Field-Based Searching of Molecular Electrostatic Potentials. *J. Chem. Inf. Comput. Sci.* **1996**, *36*, 900−908.
(105) Cheng, C.; Maggiora, G.; Lajiness, M.; Johnson, M. Four Association Coefficients for Relating Molecular Similarity Measures. *J. Chem. Inf. Comput. Sci.* **1996**, *36*, 909−915.
(106) Basak, S. C.; Grunwald, G. D. Estimation of lipophilicity from molecular structure similarity. *New J. Chem.* **1995**, *19*, 231−237.
(107) Karcher, W.; Karabunarliev, S. The Use of Computer Based Structure-Activity Relationships in the Risk Assessment of Industrial Chemicals. *J. Chem. Inf. Comput. Sci.* **1996**, *36*, 672−677.
(108) Katritzky, A. R.; Rachwal, P.; Law, K. W.; Karelson, M.; Lobanov, V. S. Prediction of Polymer Glass Transition Temperatures Using a General Quantitative Structure-Property Relationship Treatment. *J. Chem. Inf. Comput. Sci.* **1996**, *36*, 879−884.
(109) Kränz, H.; Vill, V.; Meyer, B. Prediction of Material Properties from Chemical Structures. The Clearing Temperature of Nematic Liquid Crystals Derived from Their Chemical Structures by Artificial Neural Networks. *J. Chem. Inf. Comput. Sci.* **1996**, *36*, 1173−1177.
(110) Drefahl, A. *Computable Molecular Descriptors;* Chapter 2 in ref 7.
(111) Kearsley, S. K.; Sallamack, S.; Fluder, E. M.; Andose, J. D.; Mosley, R. T.; Sheridan, R. P. Chemical Similarity Using Physicochemical Property Descriptors. *J. Chem. Inf. Comput. Sci.* **1996**, *36*, 118−127.
(112) Sheridan, R. P.; Miller, M. D.; Underwood, D. J.; Kearsley, S. K. Chemical Similarity Using Geometric Atom Pair Descriptors. *J. Chem. Inf. Comput. Sci.* **1996**, *36*, 128−136.
(113) von der Lieth, C.-W.; Stumpf-Nothof, K.; Prior, U. A Bond Flexibility Index Derived from the Constitution of Molecules. *J. Chem. Inf. Comput. Sci.* **1996**, *36*, 711−716.
(114) Basak, S. C.; Grunwald, G. D. Molecular Similarity and Risk Assessment: Analog Selection and Property Estimation Using Graph Invariants. *SAR QSAR Environ. Res.* **1994**, *2*, 289−307.
(115) Varmuza, K. K-Nearest Neighbor Classification (KNN-Method). In *Pattern Recognition in Chemistry;* Varmuza, K., Ed.; Springer-Verlag: Berlin, 1980.
(116) Drefahl, A.; Reinhard, M. Similarity-Based Search and Evaluation of Environmentally Relevant Properties for Organic Compounds in Combination with the Group Contribution Approach. *J. Chem. Inf. Comput. Sci.* **1993**, *33*, 886−895.
(117) Drefahl, A. *1-Octanol/Water Partition Coefficient;* Chapter 13 in (7), pp 13-21−13-28.
(118) Myers, D. *The Many Faces of Dodecane;* Chapter 2 in (97), pp 28−31.
(119) Kosswig, K.; Stache, H. *Die Tenside;* Carl Hanser Verlag: Munich and Vienna, 1993.
(120) Myers, D. *Micellization and Association;* Chapter 3 in (97), pp 107−116.
(121) Myers, D. *Surfactants at the Solid/Liquid Interface;* Chapter 8 in (97), pp 280−282.
(122) Surface Chemistry and Monolayers. In *The Colloidal Domain;* Evans, D. F.; Wennerström, H., Eds.; VCH Publishers, Inc.: New York, 1994.
(123) Seidel, O; Drefahl, A.; Mögel, H.-J. to be published.
(124) Klein, J.; Kamiyama, Y.; Yoshizawa, H.; Israelachvili, J. N.; Fetters, L. J.; Pincus, Modification of Long-Ranged Forces by Surface Exchange of Polymeric Amphiphiles. *Macromolecules* **1992**, *25*, 2062−2064.
(125) Foster, J. *Atomic Imaging and Positioning;* In (1), pp 15−36.
(126) Barabasi, A.-L.; Stanley, H. E. *Fractal Concepts in Surface Growth;* Cambridge University Press: Cambridge, Great Britain, 1995.
(127) Meakin, P. *Fractals and Disorderly Growth* Review; Presented at the 1989 Spring Meeting of the Materials Research Society April 24−29 (Symposium X, Frontiers of Material Research): San Diego, CA, 1989.
(128) Family, F. Scaling of rough surfaces: effects of surface diffusion. *J. Phys. A: Math. Gen.* **1986**, *19*, L441−L446.
(129) Brown, R. In *Handbook of Thin Film Technology;* Maissel, L. I., Glang, R., Eds.; McGraw-Hill, Inc.: New York, 1970.
(130) Weiss, G. H. *Aspects and Applications of the Random Walk;* North-Holland: Amsterdam, 1994.
(131) de Gennes, P.-G. *Scaling Concepts in Polymer Physics;* Cornell University Press: Ithaca and London, 1979.

CI980062X